Lattice dynamics and Raman spectrum of $BaZrO_3$ single crystals - Supplementary information

Constance Toulouse,[1,2] Danila Amoroso,[3,4,5] Cong Xin,[1,4] Philippe Veber,[6,4] Monica Ciomaga Hatnean,[7] Geetha Balakrishnan,[7] Mario Maglione,[4] Philippe Ghosez,[3] Jens Kreisel,[2] and Mael Guennou[1,2]

[1] *Materials Research and Technology Department, Luxembourg Institute of Science and Technology, 41 rue du Brill, L-4422 Belvaux, Luxembourg*

[2] *Physics and Materials Science Research Unit, University of Luxembourg, 41 Rue du Brill, L-4422 Belvaux, Luxembourg*

[3] *Theoretical Materials Physics, Quantum Materials Center (Q-MAT), Complex and Entangled Systems from Atoms to Materials (CESAM), University of Liège, Quartier Agora, Allée du Six Aout, B-4000 Liège, Belgique*

[4] *Institut de Chimie de la Matière Condensée de Bordeaux (ICMCB)- UMR 5026, 87, Avenue du Docteur Schweitzer, F-33608 Pessac, France*

[5] *National Research Council CNR-SPIN, c/o Università degli Studi "G. D'Annunzio", I-66100 Chieti, Italy*

[6] *Institut Lumière-Matière (ILM) - UMR 5306, Université Claude Bernard Lyon 1, Campus LyonTech - La Doua, 10 rue Ada Byron, F-69622 Villeurbanne, France*

[7] *Physics Department, University of Warwick, Coventry, CV4 7AL, UK*

(Dated: September 17, 2019)

Table I. Frequencies (in cm^{-1}) of the observed Raman modes at low and room temperatures in both parallel (VV) and crossed (HV) polarization configurations. In bold : the modes with higher intensity.

Low T°(4K)		Room T°		High T°(1200K)	
VV	HV	VV	HV	VV	HV
-	-	-	-	108	**113**
-	189	**193**	**190**	199	**193**
-	-	248	-	**253**	248
-	-	**277**	279	294	292
-	345	346	349	299	-
-	-	365	-	372	368
451	**455**	450	**458**	-	**482**
648	-	**639**	-	**613**	-
713	-	-	-	-	-
741	**741**	**740**	**740**	**728**	**723**
-	817	-	-	-	-
838	-	**842**	-	**843**	-
1028	-	1014	-	950	-
-	1045	-	-	-	-
1090	-	-	1065	-	-

Table II. Tables for the symmetries of phonon combinations for the cubic perovskite.

	T1u	T2u
T1u	A1g + Eg +T1g + T2g	A2g + Eg +T1g + T2g
T2u		A1g + Eg +T1g + T2g

	R1+	R3+	R4+	R4-	R5-
R1+	A1g	Eg	T1g	T1u	T2g
R3+		A1g +A2g + Eg	T1g + T2g	T1u + T2u	T1g + T2g
R4+			A1g + Eg +T1g + T2g	A1u + Eu + T1u + T2u	A1g + Eg +T1g + T2g
R4-				A1g + Eg +T1g + T2g	A1u + Eu + T1u + T2u
R5-					A1g + Eg +T1g + T2g

	X1+	X3-	X4-	X5+	X5-
X1+	A1g + Eg	T1u	T2u	T1g + T2g	T1u + T2u
X3-		A1g + Eg	A2g + Eg	T1u + T2u	T1g + T2g
X4-			A1g + Eg	T1u + T2u	T1g + T2g
X5+				A1g +A2g +2Eg +T1g +T2g	A1u +A2u +2Eu +T1u +T2u
X5-					A1g +A2g +2Eg +T1g +T2g

	M1+	M2+	M2-	M3+	M3-	M4+	M5+	M5-
M1+	A1g + Eg	A2g + Eg	A2u + Eu	T1g	T1u	T2g	T1g + T2g	T1u + T2u
M2+		A1g + Eg	A1u + Eu	T2g	T2u	T1g	T1g + T2g	T1u + T2u
M2-			A1g + Eg	T2u	T2g	T1u	T1u + T2u	T1g + T2g
M3+				A1g + Eg	A1u + Eu	A2g + Eu	T1g + T2g	T1u + T2u
M3-					A1g + Eg	A2u + Eu	T1u + T2u	T1g + T2g
M4+						A1g + Eg	T1g + T2g	T1u + T2u
M5+							A1g +A2g +2Eg +T1g +T2g	A1u +A2u +2Eu +T1u +T2u
M5-								A1g +A2g +2Eg +T1g +T2g

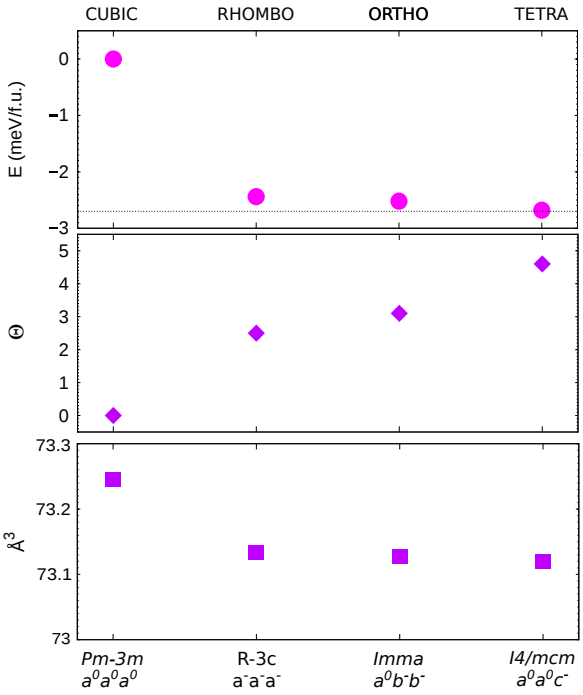

Figure 1. Calculated energy gain (in meV/f.u.), rotational angle Θ, and volume (in $Å^3$/f.u.) for T, O, and R antiferrodistortive phases of $BaZrO_3$ with respect to the cubic phase. GlazerâĂŹs notation [1] is also reported.

***I*4/*mcm*-T**				***Imma*-O**				***R*$\bar{3}$*c*-R**			
ω (cm^{-1})	mode	deg.	activity	ω (cm^{-1})	mode	deg.	activity	ω (cm^{-1})	mode	deg.	activity
23.49	E_g	2	Raman	20.01	B_{2g}	1	Raman	7.27	E_g	2	Raman
92.72	A_{1g}	1	Raman	23.02	B_{1g}	1	Raman	88.50	A_{1g}	1	Raman
101.82	E_g	2	Raman	87.07	A_g	1	Raman	98.24	A_{2g}	1	silent
104.36	B_{2g}	1	Raman	100.41	B_{2g}	1	Raman	99.34	A_{2u}	1	IR
106.52	E_u	2	IR	101.36	B_{3g}	1	Raman	104.43	E_g	2	Raman
113.38	A_{2u}	1	IR	103.75	B_{3u}	1	IR	111.66	E_u	2	IR
191.57	E_u	2	IR	106.71	B_{2u}	1	IR	187.82	E_u	2	IR
194.52	A_{2u}	1	IR	107.17	A_g	1	Raman	193.20	A_{2u}	1	IR
194.72	E_u	2	IR	114.24	B_{1u}	1	IR	194.91	E_u	2	IR
199.53	B_{1u}	1	silent	186.36	B_{3u}	1	IR	204.16	A_{1u}	1	silent
301.13	A_{1u}	1	silent	191.90	A_u	1	silent	300.89	A_{1u}	1	silent
302.03	E_u	2	IR	193.75	B_{2u}	1	IR	302.29	E_u	2	IR
356.41	E_g	2	Raman	193.85	B_{3u}	1	IR	353.29	A_{2g}	1	silent
358.05	B_{2g}	1	Raman	194.10	B_{1u}	1	IR	358.38	E_g	2	Raman
494.37	E_u	2	IR	204.40	B_{1u}	1	IR	494.27	A_{2u}	1	IR
496.48	A_{2u}	1	IR	300.73	A_u	1	silent	496.52	E_u	2	IR
534.22	A_{2g}	1	silent	302.11	B_{1u}	1	IR	535.38	E_g	2	Raman
535.33	B_{1g}	1	Raman	302.48	B_{2u}	1	IR	791.52	A_{2g}	1	silent
790.83	A_{2g}	1	silent	354.31	B_{2g}	1	Raman				
				356.37	B_{3g}	1	Raman				
				359.78	A_g	1	Raman				
				494.07	B_{3u}	1	IR				
				494.75	B_{2u}	1	IR				
				497.47	B_{1u}	1	IR				
				534.78	B_{1g}	1	Raman				
				535.53	B_{3g}	1	Raman				
				791.18	B_{3g}	1	Raman				

Table III. Calculated phonon frequencies ω (in cm^{-1}) at the Γ (0 0 0) point of the $I4/mcm$, $Imma$, and $R\bar{3}c$ Brillouin zone. The symmetry assignments in Mulliken's notation, degeneracy and activity in the infrared (IR) or Raman spectroscopy for each mode are also reported. The analysis relies on SAM [2] and SMODES [3] tools.

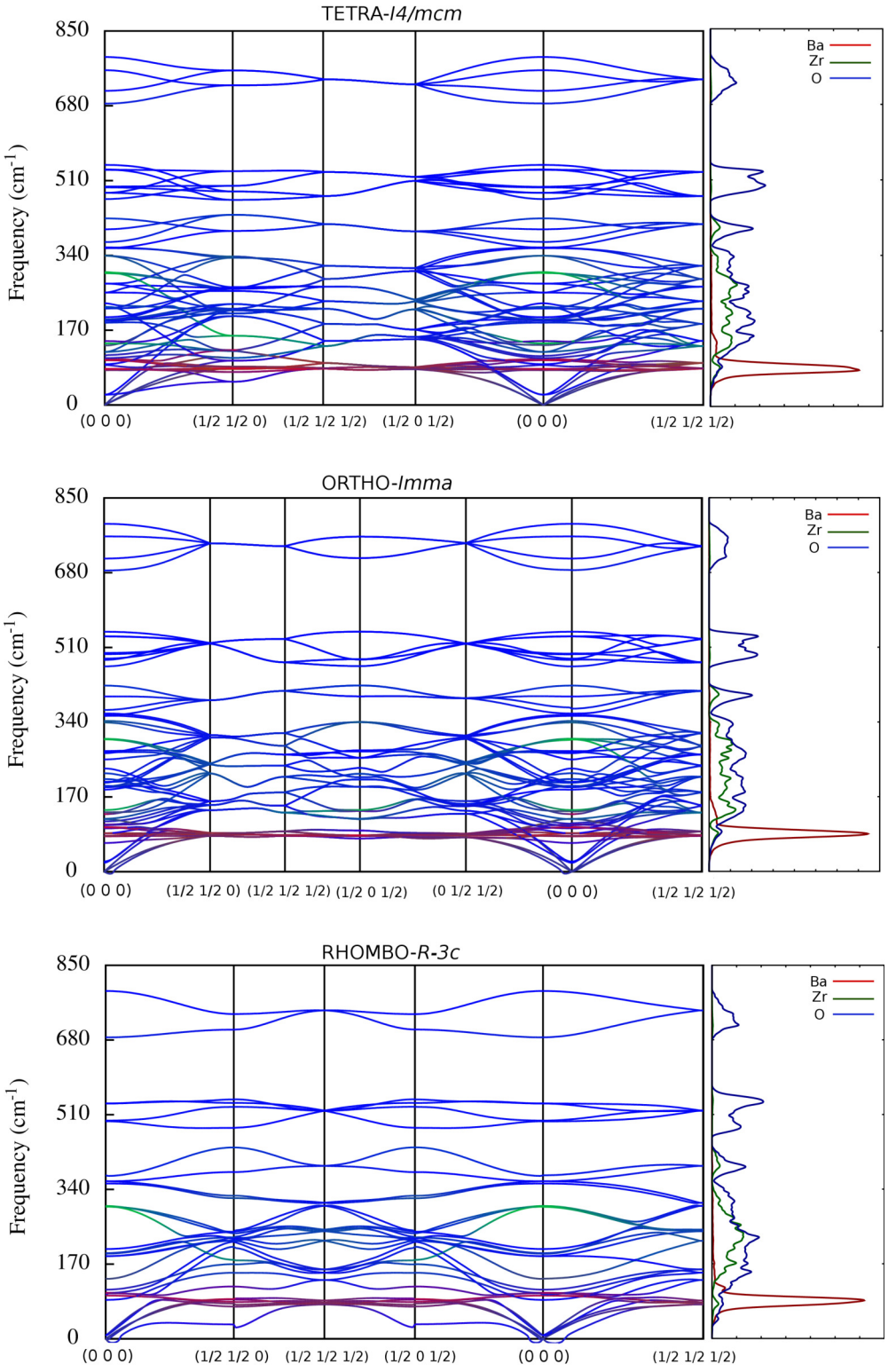

Figure 2. Calculated phonon dispersion curves of $I4/mcm$, $Imma$ and $R\bar{3}c$ antiferrodistortive structures associated to out-of-phase oxygen rotations in $BaZrO_3$. Phonon density of states by atomic species are also reported on the right side of the phonon band structures. Different colors indicate the different atomic contributions in the corresponding eigenvectors (red for the A atom, green for B atom and blue for O atoms). Calculations have been performed in the conventional 20-atom cell for the I4/mcm and Imma structures, while in the primitive 10-atom cell for the R-3c one. Small anomalies in the proximity of the high-symmetry Q-points in the phonon dispersion curves of the O and R structures are matter of accuracy in the interpolation procedure to extrapolate the curves. Therefore, they do not have physical meaning and do not affect the main aim of these graphs, that is to simply show the absence of unstable modes.

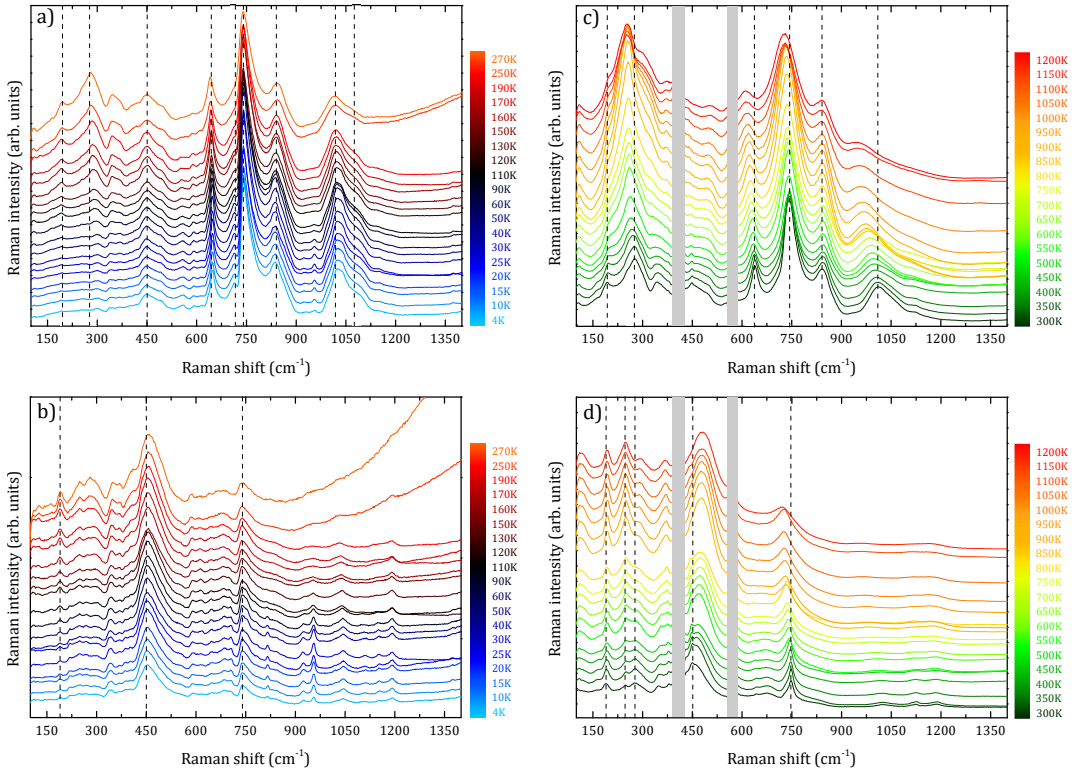

Figure 3. Temperature dependences of the polarized Raman spectra taken in parallel (a,c) and crossed (b,d) polarization configurations between 4 K and 1200 K (the spectra from 4 K to room temperature are shown on the right (a,b) whereas on the left are the spectra taken above room temperature up to 1200 K

Table IV. LO/TO polar modes frequencies (in cm^{-1}) derived from Nuzhnyy et al.[4]. The frequencies calculated in our work by DFT are shown too as a reminder.

	experimental frequencies (IR)		DFT frequencies	
Mode	TO	LO	TO	LO
Last	116	141	96	133
Slater	214	380	193	366
Axe	520	692	503	692

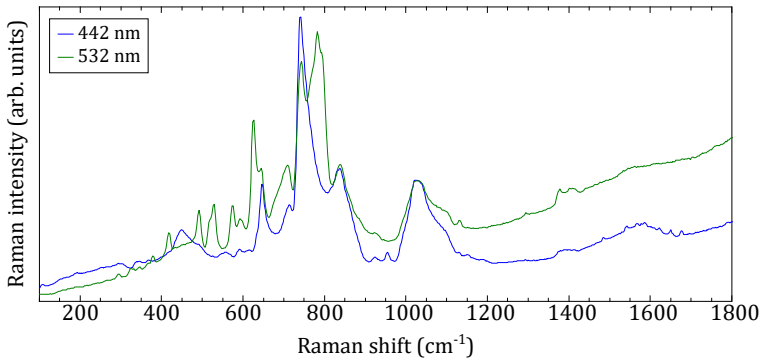

Figure 4. Polarized Raman spectra of $BaZrO_3$ taken at 10 K in parallel polarization configuration with different wavelengths of laser excitation. We can see that the small peaks visible at 925 and 955 cm^{-1} in the blue (442 nm) laser line vanish in the green (532 nm), indicating non-intrinsic signal (probably fluorescence). Conversely, an important number of parasitic peaks are observed in the green, justifying the choice of the blue laser line for our whole study.

[1] A. M. Glazer, Acta Crystallographica Section B **28**, 3384 (1972).
[2] E. Kroumova, M. Aroyo, J. Perez-Mato, A. Kirov, C. Capillas, S. Ivantchev, and H. Wondratschek, Phase Transitions **76**, 155 (2003), https://doi.org/10.1080/0141159031000076110.
[3] D. M. H. H. T. Stokes and B. J. Campbell, ISOTROPY Software Suite, iso.byu.edu .
[4] D. Nuzhnyy, J. Petzelt, M. Savinov, T. Ostapchuk, V. Bovtun, M. Kempa, J. Hlinka, V. Buscaglia, M. T. Buscaglia, and P. Nanni, Physical Review B **86**, 014106 (2012).